

1 We thank the referees for their positive and thoughtful comments.

2
3 Our responses (italics) are inline with the referee comments below. A revised manuscript
4 incorporating the described changes has been submitted.

5
6 =====

7 **Reviewer 1.**

8 =====

9 **1. General Comments**

10 The topic of this paper, correcting eddy covariance estimates of fluxes from spurious ship effects, is
11 highly topical and necessary. Air-sea interaction requires far more study, and direct measurements
12 (such as described) are essential to reduce the community dependence on derived fluxes.

13
14 I think the paper suffers from lack of rigour, edging towards the circular, although the detail of the
15 analysis is very good. This may be my relative weakness in understanding of the topic, but I would
16 then argue that if further clarity is needed for myself, then others may feel the same.

17
18 *We appreciate the reviewer's honesty and hope that the revisions described below have improved*
19 *the clarity of the paper. We do not believe the arguments presented to be in any way circular nor*
20 *lacking in rigour.*

21
22 The issue (I understand) is that an observed peak in the spectral signal of atmospheric turbulence
23 may be spurious due to ship motion, rather than inherent in the flow (e.g. eddies in the air being due
24 to air flowing over waves on the surface). Further, the observed signature is due to the motion of the
25 instrument (bolted to the ship) rather than the moving ship generating additional variable
26 diffuence.

27
28 *The reviewer is correct in their summation of the problem in the first sentence of this paragraph. The*
29 *second sentence however suggests the reviewer has misunderstood the problem – the issue is not*
30 *one of the instrument moving relative to the ship (it is rigidly mounted), nor one of diffuence*
31 *(divergence of nearby flow from the measured streamline), but of the measured streamline changing*
32 *orientation over time in response to the changing orientation of the ship. Changes to the flow over*
33 *the ship can include confluence (convergence of streamlines) as well as diffuence, though neither are*
34 *necessarily present, and are certainly not necessary as causes of the distortion observed. We provide*
35 *evidence suggesting that the source of the signature is time-varying flow distortion correlated with*
36 *the changing ship orientation..*

37
38 IF this is the overall theme of the argument (and I may be confused) then the argument may be
39 assisted by some re-arrangement of the presentation, some editing, and attention to figures.

40
41 **Some Instances**

42
43 1.1 Figure 1. A schematic positioning and flow diffuence field would be most useful here, to
44 introduce the concept (from front, side and above)The photo does not clearly indicate position of
45 sonic back from the bow point.

46
47 *A new version of Figure 1, incorporating a schematic, has been provided. The location of the sonic*
48 *anemometer relative to the ship is also given in Appendix B. The problem addressed does not relate*
49 *to diffuence per se, so illustrating this adds nothing useful to the discussion. Incorporating flow*
50 *streamline information from the CFD modeling (described in the given reference Yelland et al., 2002)*
51 *adds little. Note that the CFD model can only be run for a stationary ship, so does not allow the time-*

52 varying flow distortion to be assessed. Figure 4 illustrates the time-varying changes in the streamline
53 orientation (as illustrated by the measured tilt) with changing ship attitude.

54
55 1.2 Figure 2. Ogive does not offer much relevant information. Far ore useful would be equivalent
56 spectra from the ship accelerometers.

57
58 *The ogive is widely used within the turbulence community to assess the quality of turbulence*
59 *measurements and provides essential information – demonstrating the impact of the distortion in the*
60 *spectra on the final flux estimate. The ogive is particularly useful when assessing sample lengths for*
61 *stationarity (see comment 2.1 below), since the ogive (being a cumulative representation) is*
62 *smoother than the cospectrum.*

63
64 *The requested spectra of the ship's vertical velocity (derived from integration of the accelerometers in*
65 *the motion pack collocated with the sonic anemometer) are already given in Figure 5.b. Figure 5.d*
66 *gives cospectra of measured $\langle u'w' \rangle$ which is almost entirely dominated by the ship velocity since no*
67 *motion corrections have been applied.*

68
69 *In order to present our results more clearly, addressing both this point, point 3.3 below and point 13*
70 *from Reviewer 2, we have removed panel 5d, and added a panel to Figure 2 showing the cospectra*
71 *prior to applying motion correction (following Edson et al., 1998). This is a more appropriate point to*
72 *demonstrate the large distortions present in 'raw' cospectra.*

73
74 1.3 p 15549 line 18: "these frequencies are associated with platform motion...". This is the
75 hypothesis? Then should not be stated.

76
77 *This is not the hypothesis. The hypothesis is that "Signals in cospectra at scales associated with*
78 *waves and platform motion (the "motion-scale") result from motion error (due to...) rather than*
79 *being a turbulent signal induced by wind-wave interaction. We agree that this could be expressed*
80 *more clearly and have rewritten the sentence for clarity.*

81
82 1.4 p 15550, line 1 "Motion-scale signal can be removed..." (my italic) . Again, perhaps the issue is
83 whether it is due to
84 motion and secondarily whether it should be removed.

85
86 *We believe motion-scale signal is an appropriate term, as regardless of its source, the signal does*
87 *occur at the frequency scale of wave-induced platform motion. Whether it should be removed is the*
88 *subject of the paper. At this point in the paper we merely state that it can be removed in a*
89 *straightforward manner: discussion of whether it should be removed comes later on.*

90
91 1.5 p 15552: set of processes
92 Again, not my expertise, but I would think that a large ship such as JCR rock like a see-saw in
93 moderate waves, with a near sationarity at the centre of buoyancy (where the gyro's used to be
94 kept). How much difference is there between the observed change flow angle and the pitch of the
95 ship? This information may be in Figure 4 but the presentation is unclear. Perhaps presenting the
96 data as correlation with error of the variables against a single parameter (e.g. sensor height,
97 z_{platform}), or amplitude and phase (again with error). These data would aid the unraveling of the
98 question.

99
100 *In terms of ship's pitch only, then the see saw analogy is reasonable, as demonstrated in the*
101 *oscillation of the pitch variable in Figure 4. However, the flow angle depends not just on pitch, but*
102 *both it and the vertical platform displacement (z) and secondarily on roll and yaw and motion in the*

103 associated axes. Unraveling the exact way in which the different ship attitude/motions may impact
104 air-flow at a given point on the platform is challenging, is likely platform dependent, and beyond the
105 scope of this manuscript (which simply seeks to determine whether these motions lead to a
106 measurement error) as we state later on page 15556, lines 7/8.

107

108 We should also note that a fit to (correlation with) a single parameter (z platform, pitch, vertical
109 velocity) does not provide a unique solution for the streamline angle – the same pitch or vertical
110 displacement occurs for both positive and negative vertical velocity; the same vertical velocity occurs
111 at both positive and negative displacements from the mean. Further, because
112 acceleration/velocity/displacement are related via integration over time, and pitch similarly related
113 through the rotation about the centre of mass; the choice of independent variables is – to some
114 extent – somewhat arbitrary, as long as the pair chosen provide a unique description of the ship's
115 position/motion over time. Our choice of vertical acceleration and velocity is made based on the best
116 correlations observed, and is theoretically able to account for 'pumping' of the air over the deck
117 (forced changes of local pressure) in a way that say vertical displacement and pitch could not. This
118 point is noted in the text.

119

120 2. Specific Comments

121

122 2.1 p 15547 "Fluxes were calculated over 30 minute periods." Was any study of varying the
123 integration time to ensure stationarity attempted, especially under differing stability?

124

125 This is an important point for flux measurement, for which there is always a balance between
126 capturing the full range of turbulent contribution, and minimizing the amount of data lost to non-
127 stationarity. To ensure stationarity in our measurements, quality control criteria as described in the
128 manuscript were applied (principally the ship maneuvering criteria, and procedures detailed by Foken
129 and Wichura, 1996; Vickers and Mahrt, 1997 – as noted in the text) to remove non-stationary
130 periods. The effectiveness of these criteria has been demonstrated in many previous studies, and was
131 checked here through inspection of the low frequency limits of ogives, from which 30-minute periods
132 were deemed a suitable flux length. With regards to stability, this paper is primarily concerned with
133 moderate to high wind speeds (and the wave conditions that result from them). At winds above 6
134 m/s, all flux measurements were in unstable or near neutral conditions (here defined as $10/L < 0.2$),
135 the norm for the open ocean. At wind below 6 m/s, less than 20% of the measurements were in
136 stable conditions.

137

138 2.2 p 15548 "aligned with the mean stream line". Confirm that this sensible even for mean w
139 rotation: for instance, if flow is diffluent (with a mean updraft) do the eddies also align instantly with
140 the new wind vector?

141

142 Yes, this is sensible - this rotation into the mean streamline is standard practice in studies of air-sea
143 turbulent exchange.

144

145 2.3 p 15548 Diffluence was estimated to increase wind flow altitude by "1.3 and 3.2 m". Comment
146 on effect on stability (perhaps with ref to Froude number)

147

148 We cannot say anything about the effect of stability here – the lifting of the streamline over the ship
149 is determined via a CFD modeling study for neutral stratification. See our response to point 2.1 above
150 for general comments on stability. The primary impact of changes in stability would be to modify the
151 vertical wind speed profile. Some tests have been conducted in the past for CFD modeled flow over
152 commercial ships; even with an extreme change of profile from logarithmic to constant with altitude,
153 the impact on flow distortion was small compared with the absolute distortion.

154
155 2.4 p 15549 Comment on justification for elimination of "outliers".
156
157 *Drag coefficients above $5 \cdot 10^{-3}$ are, particularly for moderate to high wind speeds, well outside the*
158 *accepted range of physically plausible values. For the data here, limiting the measurements to our*
159 *acceptable range of relative wind directions, there were 38 measurements deemed outliers, of which*
160 *just 6 were for wind speeds of 6 m/s and greater. A note on this has been added to the text.*

161
162 2.4 p 15550 Eq 2 "MSC" should be defined early on, e.g. prior to reference to Fig 2.
163
164 *The motion-scale signal is first shown in Figure 2, and the description and correction of it both follow*
165 *from this. To improve clarity, we have added a definition of MSC to the caption for Figure 2.*

166
167 **3. Technical Corrections**

168
169 3.1 p15550 Eq 2 In general, should a wind velocity (m/s) be corrected with a mix of ship velocity (m/s
170 : OK) and acceleration (not so good)? For example, dividing by w'_{true} gives α_2 dimensionless,
171 but α_1 still has units.

172
173 *The velocity is not corrected by terms with other units. The coefficients are determined by regression,*
174 *and thus α_1 has units of s, and α_2 is dimensionless. A more physical reasoning for these units*
175 *is provided by the (equivalent) MSCf correction, where the coefficients are "defined as the ratio of*
176 *covariances of vertical wind and platform motion to variances of platform motion", ie. $\alpha_1 =$*
177 *$\langle w'_{accz} \rangle / (\text{std } accz)^2$ (units of s) and $\alpha_2 = \langle w'_{velz} \rangle / (\text{std } velz)^2$ (dimensionless), thus the*
178 *correction terms both have units of velocity.*

179
180 3.2 Figure 3. Offset each error bar group slightly in the horizontal so that over-plotting does not
181 mask data.

182
183 *We agree this figure could be clearer and have modified it accordingly.*

184
185 3.3 Figure 5. Unclear why panel 4 has -ve flux. Clarify caption

186
187 *The negative flux is only at the motion scale, and results from (uncorrected) platform motion. The y-*
188 *axis labels on Figure 5c,d were erroneously shown as f.C, when they should have been -f.C. We have*
189 *corrected the labels and altered the figure caption to clarify this (see also the response to point 13*
190 *from Reviewer 2 below). Note that the axis limits in figure 5 have be set close around the distortion*
191 *in the spectra to allow the details to be seen clearly – they are greatly 'zoomed in' compared to those*
192 *in figure 2. Please also see response to point 1.2.*

193
194 =====

195 **Reviewer 2.**

196 =====

197 **Reviewers:** Sebastian Landwehr and Brian Ward

198 **General comments:** This paper addresses the motion-correlated signal which has been observed in
199 momentum flux spectra measured on ships, even after standard motion-correction procedures have
200 been applied to the measured wind speeds. The authors present a dataset, where the motion-correlated
201 signal is relatively large, and accounts on average for 20% – 30% of the measured momentum flux
202 signal. The authors provide evidence that the peak in the motion-corrected momentum flux spec- trum
203 is not caused by wind-wave interaction, but by recirculation of the air flow at the anemometer location
204 which is caused by the push and pull of the bulky structures nearby. Further they present a simple and

205 efficient way of removing the bias.

206 We do not agree with the authors suggestion that the overestimation of momentum flux measurements
207 from ships that was reported by (Edson *et al.*, 1998) and Pedreros *et al.* (2003) should be caused by
208 the here addressed motion-correlated flow distortion. This is more likely due to the inaccurate mean
209 wind vector tilt estimation. We see the here presented decorrelation method, however, as a practical
210 approach to reduce bias in direct air-sea flux measurements. We recommend to publish this results
211 with minor revisions.

212 *We discuss the points here regarding the source of errors in previous publications in the specific*
213 *comments below.*

214 *We also note that "recirculation" of the flow is only one of the ways in which flow distortion can be*
215 *manifested and is not singled out or discussed in our manuscript. On page 15552, line 25 and page*
216 *15553 line 1 we briefly mention the possibility of vertical motion of the airflow caused by the vertical*
217 *motion of the platform, but recirculation of the airflow is unlikely to play a role at all but the lowest*
218 *wind speeds.*

219 **Specific comments:**

220 We provide specific comments below, but there are also several comments embedded in the article
221 file, which we also provide.

222 *We have corresponded with the reviewers and confirmed that all comments are listed below, and that*
223 *there is no additional article file.*

224 1. (Title) This paper deals with ship motion-induced flow distortion effects in the momentum
225 flux spectra, however, what is the motivation for “wave-induced” in the title?

226 *The ship motion and resulting biases we are concerned with is ultimately induced by wave motion.*
227 *We also want to highlight the fact that there are two possible causes for the motion scale signal and*
228 *we are trying to determine which is the case here - a real wave-induced flux component or*
229 *experimental error. Hence, we feel that this is an appropriate title.*

230 2. (Page 15545, line 1): Add the following references: O’Sullivan *et al.* (2013) and O’Sullivan
231 *et al.* (2015)

232 *We thank the reviewers for highlighting these relevant references, they have been added as*
233 *suggested.*

234 3. (Page 15545, line 14-16): This is really not surprising considering the location of your mast
235 shown in figure 1. It would appear that the flux instruments are several metres back from
236 the bow. A considerable reduction in flow distortion could be achieved by placing the
237 sensors as far forward as possible. Suggest you include a comment to this effect in the
238 conclusions.

239 *We would first note that the reviewers relate the comment cited to our installation, but it actually*
240 *relates to the findings of Weill *et al.* (2003) and Brut *et al.* (2005) for the R V Thalassa.*
241 *Nevertheless, we broadly agree with this comment and we have made some minor changes to the*
242 *conclusions section to better clarify our position on flow distortion as the potential source of the*
243 *observed bias. Locations of instrument installation are necessarily limited by the design of the ship;*
244 *while moving the instruments up and forward would minimize flow distortion, it is not technically*
245 *feasible since there is nothing to mount them on.*

246 *The ideal flux sensor location is a complicated issue, discussed fully in Yelland *et al.*, 2002*

247 (Y2002). The location of the mast on JCR is quite typical (see figs 16, 17 Y2002) and CFD
248 modelling gave typical biases compared to other ships. However, the mast itself on JCR is quite a
249 large, permanent structure whereas other ships often carry a temporary lattice mast. Similarly, the
250 foremast platform on JCR carries quite a few small-scale objects which are not included in the
251 CFD model geometry. These points are included towards the end of Section 2, and are included in
252 the Discussion section (page 15551, lines 17-22).

253 4. On (Page 15545, lines 21–24): Both *Edson et al.* (1998) and *Pedrerros et al.* (2003) show a
254 complete removal of the motion-correlated peak in the momentum flux spectra. It appears
255 therefore more likely to us, that the overestimation of the shipborne fluxes in (*Edson et al.*,
256 1998; *Pedrerros et al.*, 2003) is due to the inaccurate tilt correction, as described in
257 (*Landwehr et al.*, 2015). It is however possible that for the here presented measurements
258 the “time-varying flow distortion” is of greater importance, due to the less favourable
259 anemometer position, i.e., surrounded by bulky structures, while *Edson et al.* (1998) and
260 *Pe-dreros et al.* (2003) mounted their instrumentation in more pristine locations on slim
261 masts and close to the bow. We had originally applied a similar technique in (*Landwehr et al.*,
262 2015), but abandoned it for the final version, because one of the reviewers was not
263 willing to discuss this. For this study the reduction in the momentum flux was $\approx 6\%$. (We
264 did not publish this result in the final version)

265 *We have added a comment to the third para of section 4 (discussion) mentioning the possible*
266 *contribution of inaccurate tilt correction to the observed motion-scale signal. However, we don't*
267 *fully agree with the reviewer's assessment of the results in Edson et al (1998) and Pedrerros et al.*
268 *(2003) – it is not possible from the information in those papers to unambiguously assign remaining*
269 *bias in the flux to a particular source. Research vessels on dedicated flux experiments are often*
270 *either on-station or steaming slowly. Edson et al., (1998) restricted their flux measurements to ship*
271 *speed < 2 knots, i.e. errors due to inaccurate tilt correction would be very small. In addition Edson*
272 *et al., (1998) only show a single, noisy cospectrum, presumably not their worst. Pedrerros et al.*
273 *(2003) QCd their measurements using a ratio of $U_{rel} / \text{ship speed} > 2$ and wind direction bow-on.*
274 *This does allow inclusion of high ship speeds when the wind speed is high, but much of their data*
275 *was obtained in the vicinity of the ASIS buoy for their intercomparison. Also, at higher wind*
276 *speeds ships tend to reduce speed or go hove-to, as shown in our figure A2. The cospectra shown*
277 *by Pedrerros has a log y-axis and broad frequency bins, but even so the measured spectrum is*
278 *elevated in comparison to the ideal one for $fz/U > 0.1$, suggesting some uncorrected*
279 *contamination. Finally, the FETCH experiment took place in the Gulf of Lion, in short fetches*
280 *where sea state and ship motion would be low in the first place.*

281 *We don't claim that motion scale bias is the only issue, just a potentially significant one in*
282 *some data sets.*

283 5. (Page 15546, lines 8–10): The variation of the residual motion peaks in (*Miller et al.*, 2008) might
284 have another cause: *Miller et al.* (2008) estimated the relative orientation of their anemometer
285 and the inertial motion unit with the planar fit approach from (*Wilczak et al.*, 2001). Small
286 errors in this tilt estimation can lead to a less efficient removal of the ship motion signal. Note
287 that the magnitude of the tilt correction applied in (*Miller et al.*, 2008) was higher for the low
288 level anemometers. We had observed this effect during the preparation of (*Landwehr et al.*,
289 2015) when we applied the tilt corrections to the wind vector prior to the motion-correction.

290 *This is a good point and we have added a comment to this effect to the introduction. We have also*
291 *noted that uncertainty in the alignment of sonic and motion unit (e.g. Brooks 2008) could also*
292 *contribute.*

293 6. (Page 15548, equation 1): Note that the identification of the natural coordinate system based on a
294 single 30 minute averaging interval can be biased by possible offsets in the vertical wind
295 speed measurement, as elaborated in (*Wilczak et al.*, 2001; *Landwehr et al.*, 2015) this can

296 lead to significant errors in the tilt estimation at low wind speeds.

297 *We have added a comment to this effect to Appendix A, and have added the relevant reference*
 298 *Wilczak et al., 2001.*

299 7. (Page 15550, equation 2): Did the coefficients α_1 and α_2 show any correlation with relative wind
 300 direction or the ship speed? If such a correlation exists it could be used as an argument for
 301 your hypothesis.

302 *This is a reasonable suggestion. However, the coefficients are dependent on vertical ship motion,*
 303 *which will be correlated with ship speed, and also with relative wind direction (both ship operations,*
 304 *and platform motion are relative wind direction dependent). Hence use of the coefficient correlations*
 305 *to show the source of the signal is problematic. As we state in the manuscript, we do not attempt to*
 306 *provide a comprehensive correction, just an illustration of the problem, its potential size and likely*
 307 *cause.*

308 8. (Page 15550, lines 14–18): The observation of *Edson et al.* (1998) and *Dupuis et al.* (2003) might
 309 be more related to the wind vector tilt-estimation, see comment to (Page 15545, lines 21–24).

310 *See our response to comment 4.*

311 9. (Page 15551, lines 9–11): The agreement with the COARE 3.5 parametrisation is no argument for
 312 the in-significance of the surface currents. Do you have mea- surements or estimations of the
 313 magnitude and direction of the surface currents?

314 *Current measurements were not available for this experiment, though we anticipate that with the*
 315 *large, varied dataset we have compiled, most of the effect will average out. We have removed the*
 316 *suggestion that agreement with COARE 3.5 implies any effect is small.*

317 10. (Page 15551, lines 12–14): You could mention (*Landwehr et al.*, 2015) in this context.

318 *We have added the reference to this section (see our response to point 4) as suggested.*

319 11. (Page 15553, lines 19-21): Sharp thought!

320 12. (Page 15554, lines 23-26): This is a very strong argument.

321 13. (Page 15567, Figure 5): This is a nice illustration. You might zoom in further on the
 322 frequency range of interest. It might be worthwhile to increase the frequency resolution of the
 323 spectra, as it appears to be very close to the frequency shift that you want to show. I assume
 324 (c) and (d) show $f \cdot |C_{uw}|/u_*^2$?

325 *We thank the reviewers for these good presentation suggestions. We have zoomed in further on the*
 326 *motion scale, and the frequency resolution has been increased. Note that this resolution change*
 327 *slightly alters some of the values given on page 15554, lines 12-19, but does not affect the conclusions*
 328 *drawn from them. We have also clarified the label on 5c and 5d and altered the figure caption to*
 329 *further clarify. Panel 5d has been removed and a similar panel added to Figure 2. More details on*
 330 *this change are provided in the response to Reviewer 1 point 1.2.*

331 14. (Page 15568, Figure 6): Figure 6a shows that the average effect of the decor- relation is a
 332 reduction in CD, however in Fig. 6b it the effect is the increase the relative CD for abs(ship –
 333 relative wind direction) $> 20^\circ$ in comparison to the mea- surements where the wind was
 334 blowing bow on. What I want to say is: maybe the label in Fig. 6b should be “linear fit - CD”.

335 *The label is correct – the fit in 6a is calculated from bow on measurements (-20 to +50 degrees) and*

336 then the perturbation from that fit calculated as $[100*(drag-fit)/fit]$ for drags at all wind directions.

337 **References**

338 Dupuis, H., C. Guerin, D. Hauser, A. Weill, P. Nacass, W. M. Drennan, S. Cloché, and H. C. Graber
339 (2003), Impact of flow distortion corrections on turbulent fluxes estimated by the inertial dissipation
340 method during the fetch experiment on r/v L'atalante, *J. Geophys. Res.: Oceans*, 108(C3), 8064,
341 doi:10.1029/2001JC001075.

342 Edson, J. B., A. A. Hinton, K. E. Prada, J. E. Hare, and C. W. Fairall (1998), Direct covariance flux
343 estimates from mobile platforms at sea, *J. Atmos. Oceanic Technol.*, 15, 547–562.

344 Landwehr, S., N. O'Sullivan, and B. Ward (2015), Direct flux measurements from mobile plat-
345 forms at sea: Motion and air flow distortion corrections revisited, *J. Atmos. Oceanic Technol.*,
346 doi:10.1175/JTECH-D-14-00137.1.

347 Miller, S., T. Hristov, J. Edson, and C. Friehe (2008), Platform motion effects on measurements of
348 turbulence and air-sea exchange over the open ocean, *J. Atmos. Oceanic Technol.*, 25(9), 1683–1694.

349 O'Sullivan, N., S. Landwehr, and B. Ward (2013), Mapping flow distortion on oceanographic
350 platforms using computational fluid dynamics, *Ocean Science*, 9(5), 855–866, doi:10.5194/os-9-855-
351 2013.

352 O'Sullivan, N., S. Landwehr, and B. Ward (2015), Air-flow distortion and wave interactions: An
353 experimental and numerical comparison, *Methods Oceanogr.*, 12, 1–17, doi:10/5cw.

354 Pedreros, R., G. Dardier, H. Dupuis, H. C. Graber, W. M. Drennan, A. Weill, C. Guerin, and P.
355 Nacass (2003), Momentum and heat fluxes via eddy correlation method on the r/v L'Atalante and an
356 asis buoy, *J. Geophys. Res.*, 108, 3339.

357 Wilczak, J., S. Oncley, and S. Stage (2001), Sonic anemometer tilt correction algorithms, *Boundary-*
358 *Layer Meteorology*, 99(1), 127–150, doi:10.1023/A:1018966204465.

359

360

361

362 **Motion-correlated flow distortion and wave-induced biases**
363 **in air-sea flux measurements from ships**

364 **John Prytherch¹, Margaret J. Yelland², Ian M. Brooks¹, David J. Tupman^{1,*},**
365 **Robin W. Pascal², Bengamin I. Moat², Sarah J. Norris¹.**

367

368 [1]{ School of Earth and Environment, University of Leeds, Leeds, UK}

369 [2]{National Oceanography Centre, Southampton, UK}

370 [*]{now at Centre for Applied Geosciences, University of Tuebingen, Germany}

371

372 Correspondence to: J. Prytherch (J.Prytherch@leeds.ac.uk)

373

374
375

Abstract

376 | Direct measurements of the turbulent air-sea fluxes of momentum, heat, moisture and gases,
377 are often made using sensors mounted on ships. Ship-based turbulent wind measurements are
378 corrected for platform motion using well established techniques, but biases at scales
379 associated with wave and platform motion are often still apparent in the flux measurements.
380 It has been uncertain whether this signal is due to time-varying distortion of the air flow over
381 the platform, or to wind-wave interactions impacting the turbulence. Methods for removing
382 such motion-scale biases from scalar measurements have previously been published but their
383 application to momentum flux measurements remains controversial. Here we show that the
384 measured motion-scale bias has a dependence on the horizontal ship velocity, and that a
385 correction for it reduces the dependence of the measured momentum flux on the orientation
386 of the ship to the wind. We conclude that the bias is due to experimental error, and that time-
387 varying motion-dependent flow distortion is the likely source.

388

1. Introduction

389 Obtaining direct eddy covariance estimates of turbulent air-sea fluxes from ship-mounted
390 sensors is extremely challenging. Measurements of the turbulent wind components must be
391 corrected for the effects of platform motion and changing orientation (Edson et al., 1998;
392 Schulze et al., 2005; Brooks, 2008; Miller et al., 2008). The ship also acts as an obstacle to
393 the air flow forcing it to lift and change speed; this results in both the measured mean wind
394 being biased (accelerated/decelerated) relative to the upstream flow and the effective
395 measurement height being lower than the instrument height. This can significantly bias
396 estimates of the 10 m neutral wind speed (U_{10m}) and the surface exchange coefficients
397 (Yelland et al., 1998). Computational fluid dynamics (CFD) modelling studies of the flow
398 distortion have been used to determine corrections for these mean flow distortion effects for a
399 number of different research vessels (Yelland et al., 1998, 2002; Dupuis et al., 2003; Popinet
400 et al., 2004; Moat et al., 2005; [O'Sullivan et al., 2013, 2015](#)) and also generic corrections for
401 commercial vessels that report meteorological measurements (Moat et al., 2006a,b).
402

403 The modelled corrections show a strong dependence on the relative wind direction
404 (Yelland et al., 2002; Dupuis et al., 2003) and a much weaker dependence on wind speed, but
405 in general have been determined only for ships with zero pitch and roll angles. Weill et al.
406 (2003) and Brut et al. (2005) reported on experiments with a 1/60 scale physical model of the
407 *RV La Thalassa* to investigate the effect of pitch and roll angles on the mean flow distortion.

John Prytherch 3/9/2015 16:02

Deleted: .

409 They found the tilt of the mean streamline to vary by more than 1° and the mean wind speed
410 by up to 12% for pitch angles between $\pm 10^\circ$; these effects were asymmetric about zero pitch.
411 Roll angle had only a small impact on the measured wind speed, about 1% for roll of up to
412 10° , but this was examined for bow-on flows only and a larger impact might be expected for
413 flows with a significant beam-on component. Comparison of in situ measurements from sonic
414 anemometers, the physical model tests, and CFD modelling also revealed that the foremast
415 itself, along with the instruments and electronics enclosures mounted on it, had a significant
416 impact on flow distortion at the location of the sonic anemometer.

417 The studies of flow distortion cited above addressed only the mean flow for a fixed
418 orientation of the ship with respect to the mean streamline; to the best of our knowledge no
419 studies have investigated the effect of time-varying flow distortion as ship attitude changes.
420 That the time-varying flow distortion has an impact can, however, be inferred from reported
421 biases of ship-based eddy covariance measurements. Edson et al. (1998) compared eddy
422 covariance estimates of the kinematic wind stress from two ships with those from a small
423 catamaran and from the stable research platform FLIP. They found that the ship-based
424 estimates were on average 15% higher than those from FLIP and the catamaran. They argued
425 that the difference resulted from flow distortion over the ship rather than from inadequate
426 motion correction because the catamaran experienced more severe platform motion. Pedreros
427 et al. (2003) similarly found momentum flux estimates from a ship to be 18% higher than
428 estimates from a nearby air-sea interaction spar buoy. Evidence of such biases, ascribed to
429 flow distortion, led to the exclusion of ship-based direct flux measurements from the most
430 recent update of the COARE bulk air-sea flux algorithm (v3.5; Edson et al., 2013).

431 Features in cospectra that manifest as significant deviations from the expected
432 spectral form (e.g. Kaimal et al., 1972) at frequencies associated with waves and platform
433 motion have been reported in observations of momentum fluxes measured from FLIP (Miller
434 et al., 2008) and from fixed platforms (Deleonibus, 1971) and towers (Drennan et al., 1999).
435 A decrease in the magnitude of the feature with height led Miller et al. (2008) to ascribe its
436 source to interactions between the waves and atmospheric turbulence. The authors also note
437 that the anemometers used were not co-mounted with inertial motion units and their tilt from
438 horizontal was determined using the planar fit method; errors in the determined tilt or in
439 estimation of anemometer and inertial motion unit alignment could also contribute to the
440 observed features via incomplete correction for platform motion (Brooks, 2008; Landwehr et
441 al., 2015). Edson et al. (2013) analysed wind profile measurements from three field
442 campaigns and found little evidence of wave influence on winds at heights above 4 m in sea

ibrooks 2/9/2015 09:54

Deleted: with

444 conditions with $c_p/U_{10m} < 2.5$, where c_p is the wave phase speed. In general, reported motion-
445 scale signals in the turbulence have been observed in measurements made either at heights
446 below 10 m (Deleonibus, 1971; Miller et al., 2008) or in conditions of fast, high swell where
447 $c_p/U_{10m} \approx 2$ and $H_{swell} \gg H_{swind}$, and H_{swell} and H_{swind} are the significant wave heights of the
448 swell and wind-wave components of the wave field respectively (Drennan et al., 1999).
449 Recent results from Large Eddy Simulations over moving wave fields also suggest that, in
450 developing sea conditions waves are not expected to significantly influence turbulent winds
451 at heights of more than about 10 m (Sullivan et al., 2014). In summary, the wave field is only
452 expected to influence the turbulent winds near the surface or in conditions where swell
453 dominates the wave field.

454 High frequency gas concentration measurements for studies of air-sea exchange have
455 been shown to suffer significant motion-correlated biases resulting from the hydrostatic
456 pressure change with vertical displacement (Miller et al., 2010), and potentially from
457 mechanical sensitivities of the sensors themselves (McGillis et al., 2001; Yelland et al., 2009;
458 Miller et al., 2010). These biases cause distortions of the cospectra between the vertical wind
459 component and gas concentration (Edson et al., 2011), apparent in the cospectra at frequencies
460 associated with the platform motion, and several recent studies have applied motion
461 decorrelation algorithms to remove this signal (Miller et al., 2010; Edson et al., 2011;
462 Blomquist et al., 2014).

463 Such an approach can also correct the apparent motion-scale bias in the momentum
464 flux, but is controversial since, as discussed above, there are circumstances in which a real
465 wave-correlated signal may be expected in the turbulence measurements. Here we present
466 measurements which demonstrate a significant motion-scale feature in momentum flux
467 measurements from a research ship. We show the impact of applying a simple regression
468 procedure to remove the bias, and provide evidence that suggests the source of the bias is
469 time-varying flow distortion [correlated with ship motion and attitude](#).

470

471 2. Data

472 The measurements were made on the *RRS James Clark Ross* as part of the Waves, Aerosol
473 and Gas Exchange Study (WAGES), a programme of near-continuous measurements using
474 the autonomous AutoFlux system (Yelland et al., 2009). Turbulent wind components were
475 measured by a Gill R3 sonic anemometer installed above the forward, starboard corner of the
476 ship's foremast platform (Fig. 1). The measurement volume was approximately 16.5 m above
477 sea level. Platform motion was measured with a Systron Donner MotionPak Mk II, mounted

ibooks 2/9/2015 10:00

Deleted: ,

479 rigidly at the base of the anemometer and sampled synchronously with it. Wave field
480 measurements were made using a WAVEX X-band radar installed above the bridge top. The
481 WAVEX system obtains directional wave spectra and mean wave parameters every five
482 minutes.

483 The fast-response instrumentation operated at 20 Hz, and flux estimates were
484 calculated over 30-minute periods. The raw wind and motion measurements were first
485 despiked and the wind components corrected for platform motion using the complementary
486 filtering approach of Edson et al. (1998). The motion correction algorithm set out in Edson et
487 al. (1998) and as usually applied corrects the measured horizontal winds for low frequency
488 horizontal motions (ship's underway velocity) in the earth frame. This neglects the aliasing of
489 the ship's horizontal speed into the vertical imposed by the non-horizontal mean streamline at
490 the point of measurement due to flow distortion over the ship. The true vertical wind speed,
491 w_{true} is determined from the measured, motion-corrected vertical wind, w_{rel} , and the
492 horizontal true and relative winds (U_{true} and U_{rel}) as

493

$$494 \quad w_{true} = w_{rel} - \left(\overline{w_{rel}} \times \left[1 - \frac{\overline{U_{true}}}{\overline{U_{rel}}} \right] \right) \quad (1)$$

495

496 where overbars indicate a time average (Tupman, 2013). The derivation of Eq. (1) and the
497 impact of applying this correction are described in Appendix A. This correction addresses the
498 same source of measurement error as that recently described by Landwehr et al. (2015) who
499 address it by applying corrections for the ship's low-frequency horizontal velocity after
500 rotating the ship-relative winds (corrected for high frequency motions) into the reference
501 frame of the mean streamline for each flux averaging period.

502 After motion correction, each 30-minute record is rotated into a reference frame
503 aligned with the mean streamline, wind components were linearly detrended, and eddy
504 covariance momentum fluxes calculated. CFD modelling of the air flow over the James Clark
505 Ross was initially undertaken by Yelland et al. (2002), but only for flow on to the bow; we
506 have extended the CFD study for a much wider range of relative wind directions and the
507 results were used to determine direction-dependent corrections to the mean (30-minute
508 averaged) relative wind speed and measurement height. The new CFD study is documented
509 in Moat and Yelland (2015) and the primary results reproduced here in Appendix B. The
510 modelled wind speed bias at the sensor location varied between -0.9% and 8.4% for wind
511 directions between 20° to port of the bow and 120° to starboard, and the height by which the

512 flow was raised varied between 1.3 m and 3.2 m. Wind directions beyond 20° to port of the
513 bow were affected by small-scale obstructions on the foremast platform that are not included
514 in the CFD model; these wind directions are thus excluded from the following analysis. After
515 applying the corrections, the measured winds were corrected to 10 m height and neutral
516 stability using the Businger-Dyer relationships (Businger, 1988) and the 10 m neutral drag
517 coefficient, CD_{10m} , was calculated from U_{10m} and the momentum flux estimates.

518 The measurements used here were obtained between 09 January and 16 August, 2013
519 in locations throughout the North and South Atlantic, the Southern Ocean and the Arctic
520 Ocean, at latitudes ranging from 62°S to 75°N. After excluding measurement periods when
521 the ship was within sea ice, there were 2920 individual flux estimates available for analysis.
522 Flux estimates were then rejected from the analysis where there was excessive ship
523 manoeuvring, where flux quality control criteria were failed (Foken and Wichura, 1996;
524 Vickers and Mahrt, 1997), and when the air temperature was less than 2°C when ice build up
525 may affect the sensors. Of the remaining 1054 flux estimates, 80 were removed as outliers
526 ($CD_{10m} > 5 \times 10^{-3}$). Unless otherwise indicated, mean relative wind direction limits of 20° to
527 port, and 50° to starboard of the bow were applied, a condition met by 499 flux estimates. Of
528 the removed outliers, 38 lay within acceptable relative wind direction limits; of these, 6 were
529 at winds speeds of 6 m.s⁻¹ or greater.

531 3. Removal of the ship motion-scale signal

532 Momentum flux cospectra and ogives for U_{10m} between 10 and 14 m s⁻¹, normalised (by f/u .²
533 and $1/u$.² respectively, where f is frequency and u is the friction velocity) and averaged, are
534 shown in Fig. 2. The cospectra and ogives differ from the typical forms obtained from
535 experiments over land (e.g. Kaimal et al., 1972) at frequencies between approximately 0.06
536 and 0.25 Hz (0.09 and 0.37 in the non-dimensionalised frequency shown in Fig. 2), where a
537 significant anomalous signal is present. These are frequencies associated with surface waves
538 and with the platform motion that results, hence, we term the cospectral signal at these
539 frequencies, the motion-scale signal.

540 At wind speeds above 7 m s⁻¹, the CD_{10m} measurements are biased high compared
541 with previous results (Fig. 3). The bias relative to the eddy covariance parameterisation of
542 Smith (1980) increases, with wind speed from approximately 20% at 8 m s⁻¹ to 60% at 20 m s⁻¹.
543 Note that the Smith (1980) parameterisation was derived from eddy covariance
544 measurements made from a slim floating tower moored so as to minimise platform motion

John Prytherch 12/8/2015 13:38

Deleted: are

John Prytherch 12/8/2015 13:39

Deleted: induced by the surface waves;

John Prytherch 12/8/2015 13:39

Deleted: is signal

M.Yelland 19/8/2015 16:30

Deleted: , with t

M.Yelland 19/8/2015 16:30

Deleted: ing

550 and inducing minimal flow distortion. [The bias is smaller when compared to the COARE 3.0](#)
551 [\(Fairall et al., 2003\) or COARE 3.5 \(Edson et al., 2013\) bulk algorithms.](#)

552 The motion-scale signal can be removed from the vertical wind component, and a
553 corrected vertical wind, w_{MSC} , obtained via a simple regression method:

554
555
$$w'_{MSC} = w'_{true} - \alpha_1 acc'_z - \alpha_2 vel'_z \quad (2)$$

556
557 where acc_z and vel_z are the platform's vertical acceleration and velocity, [measured at the base](#)
558 [of the sonic anemometer](#), and primes denote fluctuations determined from Reynolds
559 decomposition. The coefficients α_1 and α_2 are determined here by regression for each 30-
560 minute flux measurement period. This algorithm, which we term the motion-scale correction
561 (MSC), is based on the regression corrections of Yelland et al., (2009) and Miller et al.,
562 (2010). It is also similar to the motion decorrelation algorithm given in a spectral formulation
563 by Edson et al. (2011), originally utilised to remove motion biases from CO₂ flux cospectra,
564 and here termed the MSC_f. The MSC_f algorithm coefficients are defined as the ratio of
565 covariances of vertical wind and platform motion to variances of platform motion. The MSC
566 and MSC_f methods give almost identical results (Fig. 2).

567 Applying the MSC algorithm removes the motion-scale signal (Fig. 2) and results in a
568 20% to 30% decrease in CD_{10n} for wind speeds above 7 m s⁻¹ and absolute values similar to
569 those of COARE [3.0 or 3.5](#) (Fig. 3). The signal removed is similar in size and of the same
570 sign as the biases in ship-based momentum flux measurements reported by Edson et al.
571 (1998) and Dupuis et al. (2003).

572 Applying the MSC to the along-wind component as well as the vertical component
573 makes an insignificant (<<1%) additional difference to the measured flux (shown as MSC_{uv}
574 in Figs. 2 and 3). Interpolating the measured cospectra across the motion-scale frequencies
575 gives similar results to the MSC algorithm under most conditions (shown as "interpolated" in
576 Figs. 2 and 3: Prytherch, 2011; Tupman, 2013). However, interpolation requires selection of
577 appropriate frequencies to interpolate between, in this case 0.04 and 0.4 Hz (0.06 and 0.59 in
578 the non-dimensionalised frequency shown in Fig. 2), and is not dependent on a physical
579 variable related to the presumed source of the error (platform motion-dependent flow
580 distortion). For these reasons, correction using the MSC algorithm is preferable.

581

582 **4. Discussion**

583 Following application of the MSC the cospectral shape matches the Kaimal form expected.
584 This suggests that the motion-scale bias is being effectively removed.

585 The MSC also results in drag coefficients that lie within the range of previous
586 parameterisations. At the highest wind speeds (over 15 m s⁻¹) the parameterisations begin to
587 diverge significantly and the WAGES CD_{10m} are larger than those given by Smith (1980) and
588 lie between those of COARE 3.0 and 3.5. It should be noted that COARE 3.0 and 3.5 are
589 both defined using wind speeds in the frame of reference of the surface currents (see
590 Appendix in Edson et al., 2013), rather than in the earth frame of reference as used by Smith
591 (1980). Surface current measurements were not available for the WAGES data. For surface
592 currents aligned with the prevailing wind direction, adopting a surface current frame of
593 reference would lead to a small apparent increase in the drag coefficients presented here.

594 While several previous studies have ascribed a high bias in drag coefficient estimates
595 from ships to flow distortion (Edson et al. 1998, 2013; Pedreros et al. 2003), they have not
596 examined the effect in detail. Inaccurate tilt estimation, a related source of error, may also
597 contribute to this bias, particularly at low wind speeds (Landwehr et al., 2015). Few other
598 studies have discussed such biases at all, and it seems likely that the severity of any motion-
599 correlated bias is highly dependent on individual platforms and instrument installations in the
600 same manner as the mean flow distortion. The bias is potentially worse here than in many
601 other studies; the sonic anemometer is mounted lower on the foremast than would be ideal
602 because the long-term measurement programme made it necessary to be able to service the
603 instruments easily and without access to a crane. There are also a greater number of small-
604 scale obstructions such as searchlights near to the measurement point than would be the case
605 on lattice style masts often deployed on dedicated flux measurement campaigns. Because the
606 measurements are continuous and autonomous, a large fraction of our data is also obtained
607 with the ship underway. In contrast, dedicated eddy covariance studies of air-sea exchange
608 would usually focus almost exclusively on measurements made on station when ship motion
609 is substantially less than when underway. Finally it is possible that such biases are present in
610 some fraction of the measurements of many studies, but are excluded from final analysis by
611 quality control procedures without a close examination of the bias being made. Many studies
612 with modest data volumes have quality controlled the individual flux estimates via a visual
613 inspection of the ogive curves, rejecting those that do not closely match the expected form
614 (e.g. Fairall et al. 1997; Norris et al. 2012).

615 As discussed in Sect. 1 above, there is evidence from previous studies that the
616 influence of the wave field on the turbulent winds should be small at heights above some

M.Yelland 19/8/2015 16:36

Deleted: the drag coefficients are in good agreement with those from the COARE 3.5 bulk algorithm and

M.Yelland 24/8/2015 10:59

Deleted: was derived using

M.Yelland 24/8/2015 10:59

Deleted: conventional

M.Yelland 24/8/2015 11:00

Deleted: (see Appendix in Edson et al., 2013).

M.Yelland 24/8/2015 11:08

Deleted: The close agreement with COARE 3.5 suggests, however, that surface currents do not, on average, significantly affect our results.

John Prytherch 26/8/2015 17:19

Deleted: ; Edson et al. 2013

627 limit which is assumed to be related to the wave properties: values between 4 and 10 m have
628 been cited (Miller et al. 2008, Sullivan et al. 2014). The Sullivan et al. (2014) results
629 correspond to a height of order 1.5 times the significant wave height. Real wave effects are
630 thus expected to be negligible for typical measurement heights of ship-based sensors (15-20
631 m) under most conditions. Below we provide more direct evidence that the wave-scale signal
632 seen in the WAGES data is due, in large part at least, to the effects of flow distortion over a
633 moving platform.

ibrooks 2/9/2015 10:24

Deleted: Here

634

635 **4.1 Motion dependence of the streamline**

636 The angle to the horizontal of the airflow measured at the sonic anemometer site was found to
637 be dependent on the vertical motion of the ship (Fig. 4). Perturbations in the tilt of the
638 streamline are approximately in phase with acc_z , out of phase with the vertical displacement
639 and pitch, and lead vel_z by about 90° . There are multiple processes that may affect the
640 streamline orientation as the ship moves over the waves:

- 641 • Vertical displacement of the ship changes the vertical extent of the obstacle that the
642 ship presents to the flow and the relative height of the measurement volume with
643 respect to that of the bow above the water line.
- 644 • The ship's pitch similarly changes both the effective size of the obstacle presented to
645 the flow and the relative location of the sonic anemometer within the distorted flow
646 above the bow.
- 647 • Vertical motion of the ship will force the overlying air to move.

648

649 In the example here for 15 m s^{-1} , bow-on winds, the airflow tilt varies by about $\pm 3^\circ$ around a
650 mean of approximately 10° . The various parameters shown in Fig. 4a are all inter-dependent,
651 but streamline tilt showed slightly more consistent trends with the velocity and acceleration
652 parameters than with displacement or pitch suggesting that "pumping" of the air above the
653 moving deck may be the dominant effect.

John Prytherch 3/9/2015 15:59

Deleted: <#>Vertical acceleration of the ship may induce vertical accelerations of the overlying air. -

654

655 **4.2 Characteristic frequencies of spectral features**

656 For a platform moving through a wave field aligned with the direction of travel, it would be
657 expected that the frequency of ship motion forced by the waves would differ from that for a
658 ship on station with no mean horizontal velocity. The change could be of either sign
659 depending on the ratio of wavelength to the length of the ship, with an increase in frequency

663 for wavelengths much longer than the ship. The measured frequency of atmospheric turbulent
 664 structures would also be shifted to higher frequencies relative to those measured when on
 665 station. The nature of the frequency shift should differ for turbulent air motions, which advect
 666 with the wind and have a ship-relative velocity equal to the sum of wind and ship speeds, and
 667 wave-correlated features in the turbulence field which are phase-locked to the surface waves
 668 (Sullivan et al. 2000; 2008; 2014), and will have a ship-relative velocity of the sum of wave-
 669 phase and ship speeds. A signal due to real wind-wave interaction should thus appear at a
 670 different frequency to that from a ship motion-induced measurement bias.

671 Figure 5 shows a comparison of the power spectral density of platform vertical
 672 velocity (S_{velz} , Fig. 5b) and frequency weighted cospectral densities for the streamwise
 673 momentum flux (normalised by u .) both for periods during which the ship was on station
 674 ($V_{ship} < 1 \text{ m s}^{-1}$, where V_{ship} is the speed of the ship) and when underway ($V_{ship} > 5 \text{ m s}^{-1}$). The
 675 cospectra are shown both before (Fig. 5d) and after (Fig. 5c) applying the standard motion
 676 correction to the measured turbulent velocity components, but without applying the MSC
 677 correction. Also shown are the spectral densities of the surface wave field (Fig. 5a). The wave
 678 radar provides wave spectra in the earth frame, corrected for ship speed; in order to compare
 679 these directly with the measured turbulence and ship-motion spectra when underway we need
 680 to transform them into a reference frame moving with the ship. This is achieved by plotting
 681 against a modified frequency, $f_m = f_0(c_p + V_{ship})/c_p$, where f_m is the frequency that would be
 682 measured in the ship reference frame and f_0 is the true frequency in the earth frame. The
 683 periods chosen all have bow-on winds, wind speeds of between 10 and 12 m s^{-1} and similar
 684 sea states: the (true) mean peaks of the mean WAVEX-derived non-directional wave spectra
 685 (S_{wave}) are 0.120 and 0.110 Hz, and mean significant wave heights are 4.73 m and 3.51 m for
 686 the stationary and underway periods respectively.

687 For the on station measurements, the peak in the momentum flux cospectra (no MSC,
 688 Fig. 5c) is at 0.113 Hz, which matches that of the peak in ship vertical velocity (Fig. 5b) and
 689 is at slightly lower frequency than the peak in the ship-frame surface wave spectra (0.120 Hz,
 690 Fig. 5a). For the underway cases the peak in the ship-frame wave spectra is shifted to higher
 691 frequency (0.163 Hz) compared to the true spectra. The peak in the ship motion spectrum
 692 (0.148 Hz) is again lower than that of the wave spectrum and by a larger margin than for the
 693 on station case. The peak in the momentum flux cospectrum at 0.153 Hz is much closer to
 694 that of the ship motion than that of the wave spectrum.
 695 The correspondence of the peak in momentum flux cospectra with that of the ship

John Prytherch 13/8/2015 15:57

Deleted: 5

John Prytherch 3/9/2015 16:01

Deleted: The peak in the cospectra prior to motion correction (Fig. 5d) is at a slightly higher frequency (0.125 Hz) than that of the waves.

John Prytherch 13/8/2015 15:58

Deleted: 5

John Prytherch 13/8/2015 15:59

Deleted: Again,

John Prytherch 13/8/2015 15:59

Deleted: the peak in the momentum flux cospectrum matches that of the ship motion. The peak in the cospectrum prior to motion correction at 0.155 Hz, much closer to the that of the ship motion than the wave spectrum

John Prytherch 13/8/2015 16:01

Deleted: lies between those of the modified wave spectrum and ship motion.

709 motion rather than that of the wave field suggest that the residual signal after motion
710 correction is an artefact of motion-correlated flow distortion rather than a result of a real
711 wave-correlated signal in the turbulence.

712

713 **4.3 Directional dependence of drag coefficient bias**

714 Mean flow distortion is strongly dependent on relative wind direction (Yelland et al., 1998),
715 even for a motionless ship with zero pitch and roll angles. The dependence of the calculated
716 drag coefficients on relative wind direction before and after applying the MSC algorithm is
717 shown in Fig. 6. First, a linear fit was made between the drag coefficient and wind speed data
718 obtained for wind directions between -20 and +50 degrees of the bow. Then the drag
719 coefficient anomalies (individual minus fit) were calculated and averaged into 10° relative
720 wind direction bins, and the results were plotted against relative wind direction. It can be seen
721 that prior to applying the MSC algorithm the drag coefficient anomalies have a significant
722 dependence on relative wind direction, and that application of the algorithm significantly
723 reduces this dependence. For completeness the results are also shown without first applying
724 the direction-dependent CFD-derived correction to the mean, 30-minute averaged, wind
725 speed; this also reduces the dependence of the drag coefficient on relative wind direction.

726 Application of the MSC and the mean CFD correction does not completely remove all
727 dependence of the drag coefficient on relative wind direction. This suggests that one or both
728 corrections may need refinement. In the case of the MSC algorithm, the effect of the roll of
729 the ship is likely to become significant when the wind direction is beam-on rather than bow-
730 on. In the case of the CFD correction to the mean wind speed, the model of the ship geometry
731 may have to be refined to take into account local flow distortion caused by small objects
732 mounted on the foremast, close to the anemometer. These are areas for future investigation.

733

734 **5. Conclusions**

735 Methods for removal of motion-correlated signals from fast-response gas measurements
736 made onboard moving platforms have become more commonly applied in recent years;
737 however, these techniques remain controversial when applied to fast-response winds for the
738 purpose of momentum flux calculation. The results here demonstrate these methods and their
739 impact on ship-based momentum flux measurements where a significant motion-correlated
740 bias is present in the motion-corrected cospectra. The motion-correlated signals are shown to
741 be dependent on platform velocity relative to the wave field. In addition, the dependence of
742 the flux on wind direction relative to the ship is reduced after applying the correction

743 methods. These results suggest that the motion-correlated signal is due to the effects of time-
744 varying flow distortion. Further investigation is required to resolve the details of the physical
745 processes involved.

746 The recent revision of the COARE bulk flux algorithm (COARE 3.5, Edson et al.
747 2013) is determined only from data from platforms other than ships (buoys, towers, FLIP).
748 These data all require motion correction, and Bigorre et al. (2013) report biases of a few
749 percent in mean wind speed due to flow distortion around one of the buoys used to collect
750 data at high wind speed, but these platforms generally do not suffer such significant flow
751 distortion problems as ships.

752 For many applications, ship-based measurements are the only option; for example,
753 direct eddy covariance measurements of gas transfer require instrumentation that can only
754 realistically be operated on a ship. A means of effectively dealing with biases induced by
755 flow distortion around a moving platform is thus essential. The methods demonstrated above
756 provide a successful correction; after its application the shape of the cospectra matches the
757 Kaimal form expected and our drag coefficient results lie within the range of recent leading
758 parameterisations.

760 Appendix A. Underway vertical wind speed

761 The motion correction algorithm of Edson et al. (1998) calculates a total platform velocity in
762 the earth frame as the sum of highpass filtered wave-induced motions, obtained from the
763 integration of accelerometers, and lowpass filtered velocities (the platform's underway
764 motion). The latter are applied only in the horizontal since the mean vertical velocity is zero
765 by definition. The corrected winds in the earth frame are obtained as the vector sum of
766 measured and platform velocities. This neglects the impact of flow distortion on the measured
767 winds (Fig. A1). At the point of measurement on the foremast of a ship, the mean flow is
768 forced to lift resulting in a streamline tilted upwards from the horizontal. The measured
769 along-streamline wind depends upon ship velocity as well as earth-relative wind. Since the
770 streamline is tilted, a fraction of the ship velocity affects the measured vertical as well as the
771 horizontal winds in the earth frame and must be corrected.

772 When conditions are stationary (an implicit assumption for direct flux measurement)
773 the measured, motion-corrected vertical wind, w_{rel} , can be corrected for the horizontal
774 platform mean velocity to obtain the true vertical wind speed w_{true} . The ratio of the mean true
775 to mean relative vertical winds is equal to the ratio of the mean true to mean relative
776 horizontal winds, i.e.

John Prytherch 26/8/2015 19:45

Deleted: .

M.Yelland 24/8/2015 11:24

Deleted: Ship measurements were excluded from the COARE 3.5 development explicitly because of evidence of the potential for biases resulting from flow distortion.

M.Yelland 19/8/2015 17:31

Deleted: however,

M.Yelland 24/8/2015 11:14

Deleted: agree with COARE 3.5

ibrooks 2/9/2015 11:08

Deleted: previous

M.Yelland 19/8/2015 17:33

Deleted: .

786

787

$$\frac{\overline{U_{true}}}{\overline{U_{rel}}} = \frac{\overline{w_{true}}}{\overline{w_{rel}}} \quad (\text{A1})$$

788

789 (Fig. A1). Then, as

790

791

$$w_{true} = w_{rel} - (\overline{w_{rel}} - \overline{w_{true}}) \quad (\text{A2})$$

792

793 w_{true} can be determined via Eq. (1)

794

795

$$w_{true} = w_{rel} - (\overline{w_{rel}} \times [1 - \overline{U_{true}} / \overline{U_{rel}}]).$$

796

797 Note that this affects the mean vertical wind only, not the high frequency perturbations;

798 however failure to account for the impact of flow distortion on the vertical wind

799 measurements would result in the streamline orientation being incorrectly calculated, and

800 both u' and w' values being biased after rotation into the streamline-oriented reference frame

801 in which the fluxes are calculated. We also note that at low wind speeds ($\sim < 5 \text{ m s}^{-1}$), the

802 determination of the reference frame for a particular measurement interval may be biased by

803 offsets in the vertical wind speed, leading to errors in the tilt calculation (Wilczak et al.,

804 2001; Landwehr et al., 2015).

805 The effectiveness of this correction is demonstrated through comparison of drag

806 coefficients from periods when the ship was stationary ($V_{ship} < 1 \text{ m s}^{-1}$) and underway ($V_{ship} >$

807 5 m s^{-1}). Prior to correction, measurements from the underway ship are biased high relative to

808 the stationary measurements (Fig. A2). Following correction, the stationary and underway

809 measurements are in very good agreement for all but the very lowest wind speeds.

810 Furthermore, for stationary periods (where the effect is small), the corrected and uncorrected

811 results are also in good agreement.

812

813 **Appendix B. CFD corrections for flow distortion**

814 The relative wind direction dependent CFD corrections for the mean flow distortion over the

815 ship are given in Table B1. These are strictly valid only for the location of our sonic

816 anemometer (1.24 m to starboard, 16.5 m above the waterline, and 5.0 m aft of the bow), but

817 should be broadly representative for nearby locations, and indicative of the directionally
818 dependent flow distortion that might be expected on any similar installation on other ships.

819

820 **Acknowledgements**

821 WAGES was funded by the Natural Environment Research Council (grant numbers
822 NE/G00353X/1 and NE/G003696/1). We would like to thank the two captains and crews of
823 the *RRS James Clark Ross* and the ship logistics support staff at the British Antarctic Survey
824 for their help throughout the project.

825

826 **References**

827 [Bigorre, S. P., Weller, R. A., Edson, J. B. and Ware, J. D.: A Surface Mooring for Air–Sea
828 \[Interaction Research in the Gulf Stream. Part II: Analysis of the Observations and Their
829 \\[Accuracies. J. Atmos. Oceanic Technol.\\]\\(#\\), 30, 450–469.
830 \\[doi: http://dx.doi.org/10.1175/JTECH-D-12-00078.1. 2013\\]\\(#\\)\]\(#\)](#)

831 Blomquist, B. W., Huebert, B. J., Fairall, C. W., Bariteau, L., Edson, J. B., Hare, J. E., and
832 McGillis, W. R.: Advances in air-sea CO₂ flux measurement by eddy correlation,
833 Bound.-Lay. Meteorol. 1-32, doi:10.1007/s10546-014-9926-2, 2014.

834 Brooks, I. M.: Spatially Distributed Measurements of Platform Motion for the Correction of
835 Ship-Based Turbulent Fluxes. *J. Atmos. Ocean. Tech.*, 25, 2007-2017,
836 doi:10.1175/2008JTECHA1086.1, 2008.

837 Brut, A., Butet, A., Durand, P., Caniaux, G., and Planton, S.: Air–sea exchanges in the
838 equatorial area from the EQUALANT99 dataset: Bulk parameterizations of turbulent
839 fluxes corrected for airflow distortion, *Q. J. Roy. Meteor. Soc.*, 131, 2497-2538,
840 doi:10.1256/qj.03.185, 2005.

841 Businger, J. A.: A note on the Businger–Dyer profiles. *Bound.-Lay. Meteorol.*, 42, 145–151,
842 doi:10.1007/978-94-009-2935-7_11, 1988.

843 Deleonibus, P.: Momentum flux and wave spectra observations from an ocean tower. *J.*
844 *Geophys. Res.*, 76, 6506-6527, doi:10.1029/JC076i027p06506, 1971.

845 Drennan, W., Kahma, K., and Donelan, M.: On momentum flux and velocity spectra over
846 waves. *Bound.-Lay. Meteorol.*, 92, 489-515, doi:10.1023/A:1002054820455, 1999.

847 Dupuis, H., Geurin, D., Hauser, D., Weill, A., Nacass, P., Drennan, W.M., Cloche, S. and
848 Graber, H.C.: Impact of flow distortion corrections on turbulent fluxes estimated by the
849 inertial dissipation method during the FETCH experiment on R/V L’Atalante, *J.*
850 *Geophys. Res.*, 108, 8064, doi:10.1029/2001JC001075, 2003.

851 Edson, J. B., Hinton, A. A., Prada, K. E., Hare, J. E., and Fairall, C. W.: Direct covariance
852 flux estimates from mobile platforms at sea, *J. Atmos. Ocean. Tech.*, 15, 547-562,
853 doi:10.1175/1520-0426(1998)015<0547:DCFEFM>2.0.CO;2, 1998.

854 Edson, J. B., Fairall, C. W., Bariteau, L., Zappa, C. J., Cifuentes-Lorenzen, A., McGillis, W.
855 R., Pezoa, S., Hare, J. E., and Helmig, D.: Direct covariance measurement of CO₂ gas
856 transfer velocity during the 2008 Southern Ocean Gas Exchange Experiment: Wind
857 speed dependency, *J. Geophys. Res.*, 116, C00F10, doi:10.1029/2011JC007022, 2011.

858 Edson, J. B., Venkata Jampana, V., Weller, R. A., Bigorre, S. P., Plueddemann, A. J., Fairall,
859 C. W., Miller, S. D., Mahrt, L., Vickers, D., and Hersbach, H.: On the exchange of
860 momentum over the open ocean. *J. Phys. Oceanogr.*, 43, 1589–1610, doi:10.1175/JPO-
861 D-12-0173.1, 2013.

862 Fairall, C. W., White, A. B., Edson, J. B., and Hare, J. E.: Integrated shipboard measurements
863 of the marine boundary layer, *J. Atmos. Ocean. Tech.*, 14, 338–359, doi:10.1175/1520-
864 0426(1997)014<0338:ISMOTM>2.0.CO;2, 1997.

865 [Fairall, C. W., Bradley, E. F., Hare, J. E., Grachev, A. A., and Edson J. B.: Bulk](#)
866 [parameterization of air-sea fluxes: Updates and verification for the COARE algorithm,](#)
867 [J. Clim., 16, 571–591, doi:10.1175/1520-0442, 2003](#)

868 Foken, T., and Wichura, B.: Tools for quality assessment of surface-based flux measurements
869 1. *Agr. Forest Meteorol.*, 78, 83-105, doi:10.1016/0168-1923(95)02248-1, 1996.

870 Kaimal, J. C., Izumi, Y. J., Wyngaard, C., and Cote, R.: Spectral characteristics of surface-
871 layer turbulence, *Q. J. Roy. Meteor. Soc.*, 98 (417), 563-589,
872 doi:10.1002/qj.49709841707, 1972.

873 Landwehr, S., O’Sullivan, N., and Ward, B.: Direct Flux Measurements from Mobile
874 Platforms at Sea: Motion and Air-Flow Distortion Corrections Revisited, *J. Atmos.*
875 *Ocean. Tech.*, (in press), doi:10.1175/JTECH-D-14-00137.1, 2015.

876 McGillis, W. R., Edson, J. B., Hare, J. E., and Fairall, C. W.: Direct covariance air-sea CO₂
877 fluxes. *J. Geophys. Res.-Oceans*, 106, 16729-16745, doi:10.1029/2000JC000506, 2001.

878 Miller, S. D., Hristov, T. S., Edson, J. B., and Friehe, C. A.: Platform motion effects on
879 measurements of turbulence and air-sea exchange over the open ocean, *J. Atmos. Ocean.*
880 *Tech.*, 25, 1683-1694, doi:10.1175/2008JTECHO547.1, 2008.

881 Miller, S. D., Marandino, C., and Saltzman, E. S.: Ship-based measurement of air- sea CO₂
882 exchange by eddy covariance. *J. Geophys. Res.-Atmos.*, 115, D02304,
883 doi:10.1029/2009JD012193, 2010.

884 Moat, B. I., Yelland, M. J., Pascal, R. W., and Molland, A. F.: An overview of the airflow

885 distortion at anemometer sites on ships, *Int. J. Climatol.*, 25(7), 997-1006,
886 doi:10.1002/joc.1177, 2005.

887 Moat, B. I., Yelland, M. J., Pascal, R. W., and Molland, A.F.: Quantifying the airflow
888 distortion over merchant ships. Part I: validation of a CFD model, *J. Atmos. Ocean.*
889 *Tech.*, 23(3), 341-350, doi:10.1175/JTECH1858.1, 2006a.

890 Moat, B. I., Yelland, M. J., and Molland, A. F.: Quantifying the airflow distortion over
891 merchant ships. Part II: application of the model results, *J. Atmos. Ocean. Tech.*, 23(3),
892 351-360, doi:10.1175/JTECH1859.1, 2006b.

893 Moat, B. I. and Yelland, M. J.: Airflow distortion at instrument sites on the RRS James Clark
894 Ross during the WAGES project. National Oceanography Centre, Southampton, U.K.
895 Internal Document No. 12. Available from <http://eprints.soton.ac.uk/373216/>, 2015.

896 Norris, S. J., Brooks, I. M., Hill, M. K., Brooks, B. J., Smith, M. H., and Sproson, D. A. J.:
897 Eddy Covariance Measurements of the Sea Spray Aerosol Flux over the Open Ocean. *J.*
898 *Geophys. Res.*, 117, D07210, 15pp, doi:10.1029/2011JD016549, 2012.

899 [O'Sullivan, N., Landwehr, S., and Ward, B.: Mapping flow distortion on oceanographic](#)
900 [platforms using computational fluid dynamics. *Ocean Science*, 9\(5\), 855–866,](#)
901 [doi:10.5194/os-9-855-2013, 2013.](#)

902 [O'Sullivan, N., Landwehr, S., and Ward, B.: Air-flow distortion and wave interactions: An](#)
903 [experimental and numerical comparison. *Methods Oceanogr.*, 12, 1–17,](#)
904 [doi:10.1016/j.mio.2015.03.001, 2015.](#)

905 Pedreros, R., Dardier, G., Dupuis, H., Graber, H. C., Drennan, W. M., Weill, A., Geurin, C.,
906 and Nacass, P.: Momentum and heat fluxes via the eddy correlation method on the R/V
907 L'Atalante and an ASIS buoy, *J. Geophys. Res.*, 108, C11, doi:10.1029/2002JC001449,
908 2003.

909 Popinet, S., Smith, M., and Stevens, C.: Experimental and numerical study of turbulence
910 characteristics of airflow around a research vessel, *J. Atmos. Ocean. Tech.*, 21, 1575-
911 1589, doi:10.1175/1520-0426(2004)021<1575:EANSOT>2.0.CO;2, 2004.

912 Prytherch, J.: Measurement and parameterisation of the air-sea CO₂ flux in high winds. PhD
913 thesis, University of Southampton, 2011.

914 Schulze, E. W., Sanderson, B. G., and Bradley, E. F.: Motion correction for shipborne
915 turbulence sensors. *J. Atmos. Ocean. Tech.*, 22, 44-69, doi:10.1175/JTECH-1685.1,
916 2005.

917 Smith, S.: Wind stress and heat flux over the ocean in gale force winds. *J. Phys. Oceanogr.*,
918 10, 709–726, doi:10.1175/1520-0485(1980)010<0709:WSAHFO>2.0.CO;2, 1980.

919 Sullivan, P. P., McWilliams, J. C., and Moeng, C.-H.: Simulation of turbulent flow over
920 idealized water waves, *J. Fluid. Mech.*, 404, 47-85, doi:10.1017/S0022112099006965,
921 2000.

922 Sullivan, P. P., Edson, J. B., Hristov, T., and McWilliams, J. C.: Large-eddy simulations and
923 observations of atmospheric marine boundary layers above non-equilibrium surface
924 waves, *J. Atmos. Sci.*, 65, 1225-1245, doi:10.1175/2007JAS2427.1, 2008.

925 Sullivan, P. P., McWilliams, J. C., and Patton, E. G.: Large-Eddy Simulation of Marine
926 Atmospheric Boundary Layers above a Spectrum of Moving Waves. *J. Atmos. Sci.*, 71,
927 4001–4027. doi:10.1175/JAS-D-14-0095.1, 2014.

928 Tupman, D. J.: Air-sea flux measurements over the Southern Ocean. PhD thesis, University
929 of Leeds, 2013.

930 Vickers, D., and Mahrt, L.: Quality control and flux sampling problems for tower and aircraft
931 data. *J. Atmos. Ocean. Tech.*, 14, 512-526, doi:10.1175/1520-
932 0426(1997)014<0512:QCAFSP>2.0.CO;2, 1997.

933 Weill, A., Eymard, L., Caniaux, G., Hauser, D., Planton, S., Dupuis, H., Brut, A., Guerin, C.,
934 Nacass, P., Butet, A., Cloché, S., Perderos, R., Durand, P., Bourras, D., Giordani, H.,
935 Lachaud, G., and Bouhours, G.: Toward a Better Determination of Turbulent Air–Sea
936 Fluxes from Several Experiments, *J. Climate*, 16, 600-618, doi:10.1175/1520-
937 0442(2003)016<0600:TABDOT>2.0.CO;2, 2003.

938 [Wilczak, J., Oncley, S. and Stage, S.: Sonic anemometer tilt correction algorithms, *Bound.-*
939 *Lay. Meteorol.*, 99\(1\), 127–150, doi:10.1023/A:1018966204465, 2001.](#)

940 Yelland, M. J., Moat, B. I., Taylor, P. K., Pascal, R.W., Hutchings, J. and Cornell, V. C.:
941 Wind stress measurements from the open ocean corrected for airflow distortion by the
942 ship, *J. Atmos. Ocean. Tech.*, 28, 1511-1526, doi:10.1175/1520-
943 0485(1998)028<1511:WSMFTO>2.0.CO;2, 1998.

944 Yelland, M. J., Moat, B. I., Pascal, R. W., and Berry, D. I.: CFD model estimates of the
945 airflow distortion over research ships and the impact on momentum flux measurements,
946 *J. Atmos. Ocean. Tech.*, 19, 1477-1499, doi:10.1175/1520-
947 0426(2002)019<1477:CMEOTA>2.0.CO;2, 2002.

948 Yelland, M., Pascal, R., Taylor, P. and Moat, B.: AutoFlux: an autonomous system for the
949 direct measurement of the air-sea fluxes of CO₂, heat and momentum. *J. Operation.*
950 *Oceanogr.*, 15-23, doi:10.1080/1755876X.2009.11020105, 2009.

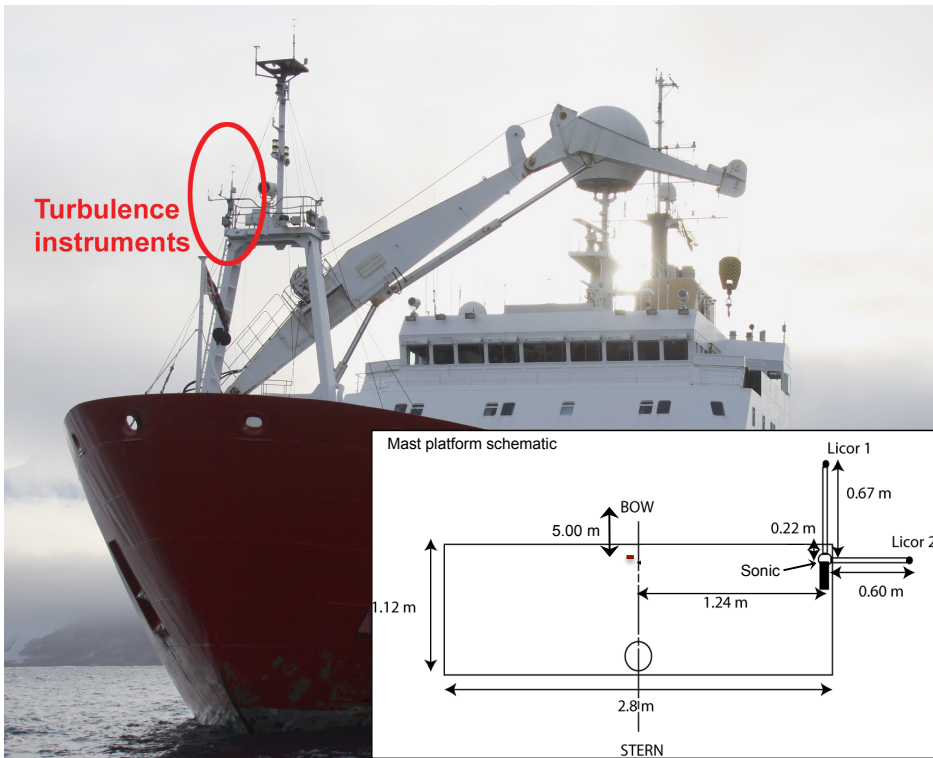
951

952

Relative wind direction (°)	wind speed bias at $z - \Delta z$ (%)	Δz (m)
-20	2.98	1.44
-10	0.41	1.35
0	-0.39	1.32
10	-0.86	1.41
20	0.7	1.54
30	2.92	1.76
50	5.11	2.27
70	4.86	2.73
90	8.35	2.96
110	6.97	3.15

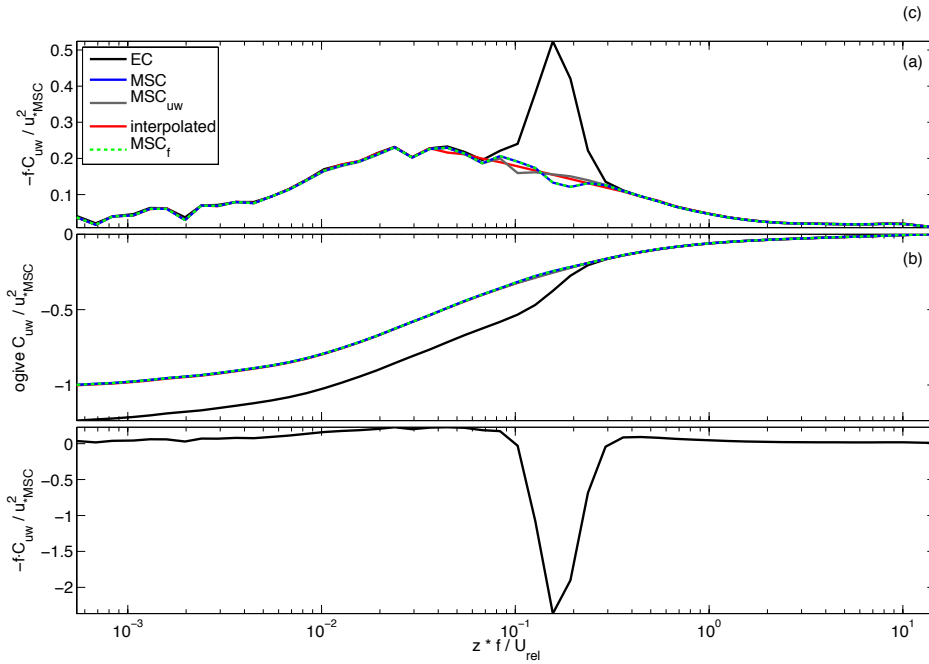
953

954 Table B1. Variation of wind speed bias and vertical flow displacement with relative wind
955 direction, determined at the location of the AutoFlux anemometer (height above sea level, z ,
956 16.5 m). The wind speed bias and Δz are relative to a free stream location 2 seconds upstream
957 of the anemometer site (after Yelland et al., 2002). A negative relative wind direction
958 indicates a flow over the port side. Further details are given in Moat and Yelland (2015).
959

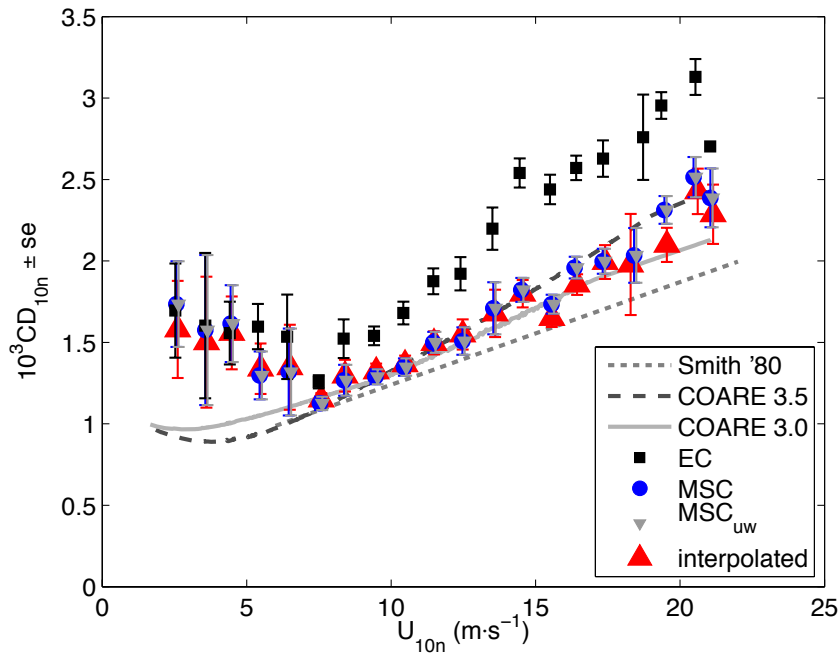


960
 961 Figure 1. Locations of the flux instrumentation on the *RRS James Clark Ross*. The sonic
 962 anemometer is 2.0 m above the starboard forward corner of the platform. Note that the
 963 foremastle crane is generally stowed close to the deck while the ship is underway or on
 964 station.

965



966
 967 Figure 2. Frequency-weighted and normalised momentum flux cospectra (a) and normalised
 968 ogives (b), shown relative to frequency non-dimensionalised using measurement height z and
 969 mean relative wind speed U_{rel} . Also shown are frequency-weighted, inverted and normalised
 970 cospectra calculated prior to motion correcting the turbulent velocity components, which
 971 results in a large upwards flux signal at the motion scale (c). Results shown are an average of
 972 131 30-minute duration measurements at mean wind speeds $10 \text{ m s}^{-1} < U_{10m} < 14 \text{ m s}^{-1}$. EC
 973 indicates the cospectra after removing platform motion following Edson et al. (1998) and
 974 shows the residual signal at scales typical of the wave field. The interpolation across the
 975 wave scales has been applied between frequencies of 0.04 and 0.4 Hz. The motion-scale
 976 correction (MSC) can either be applied as per Eq. (2) (MSC), with Eq. (2) applied to both the
 977 along and vertical wind components (MSC_{uw}), or as described by Edson et al., (2011)
 978 (MSC_f). Normalisation of the five different sets of results is by u_* with MSC applied as per
 979 Eq. (2). Note that the MSC_f line overlies the MSC line at all frequencies, and the
 980 interpolated, MSC_{uw} and EC lines for frequencies away from the motion-scale.



982

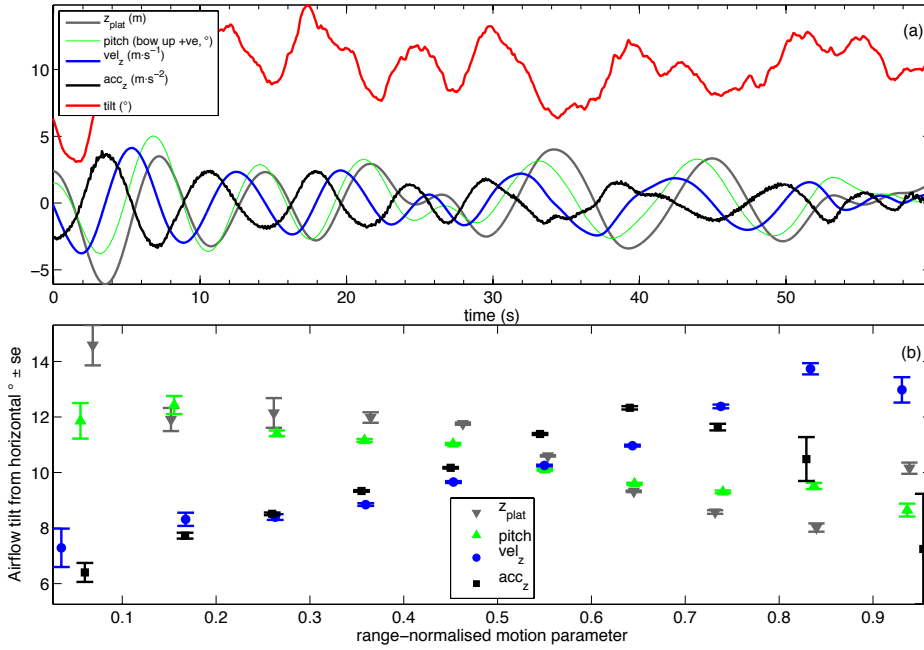
983 Figure 3. Drag coefficients bin-averaged by wind speed, relative to U_{10n} ($n = 499$).984 Measurements are shown either without correction for wave-scale bias (EC), or with
985 correction applied to the vertical velocity only (MSC), both vertical and horizontal velocity986 components (MSC_{uw}), or via a simple interpolation across the wave-scale portion of the

987 | cospectra (interpolated). The bulk COARE 3.0 and 3.5 results are calculated without

988 dependence on wave field or radiation.

John Prytherch 3/9/2015 16:06

Deleted: (Edson et al., 2013)

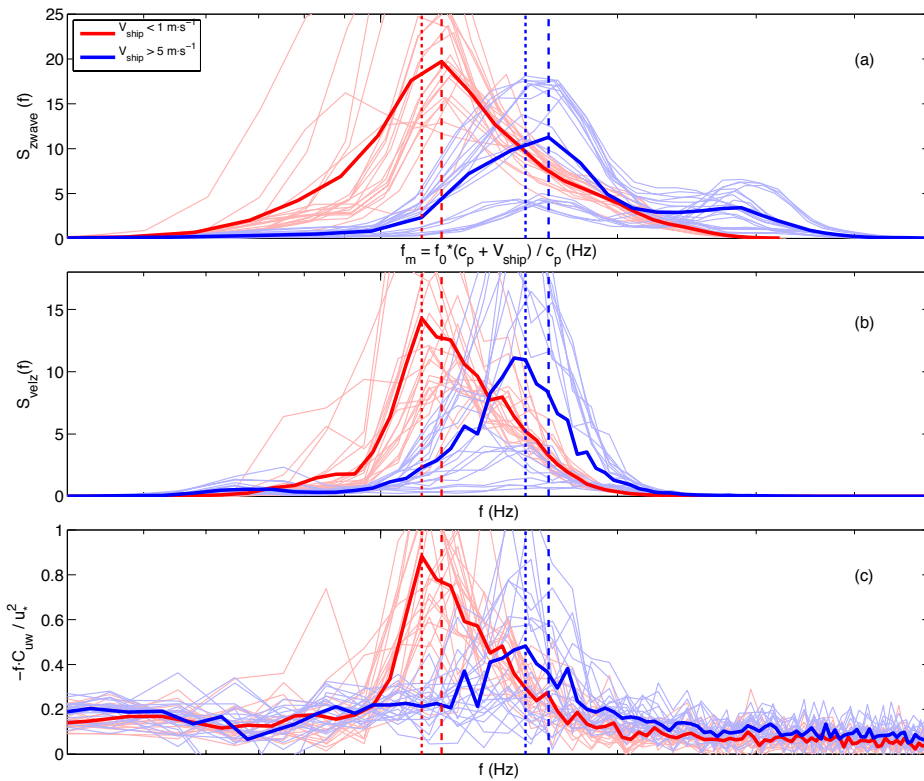


991

992 Figure 4. (a): Time series (60 s) of vertical platform displacement, velocity and acceleration,
 993 platform pitch, and tilt from horizontal of the streamwise airflow measured by the AutoFlux
 994 anemometer. The tilt has been smoothed with a 40-sample moving average. The
 995 measurements are sampled from a period (23 April 2013, 21:00-21:30 UTC) with near bow-
 996 on winds and mean U_{10m} of 15.2 m s⁻¹. (b): Variation of the tilt of streamwise airflow from
 997 horizontal, relative to the vertical platform displacement, velocity, acceleration and platform
 998 pitch each normalised by their measured range. Tilt averages were made over the 30-minute
 999 period that the measurements in (a) were sampled from.

1000

1001



1002

1003

1004

1005

1006

1007

1008

1009

1010

1011

1012

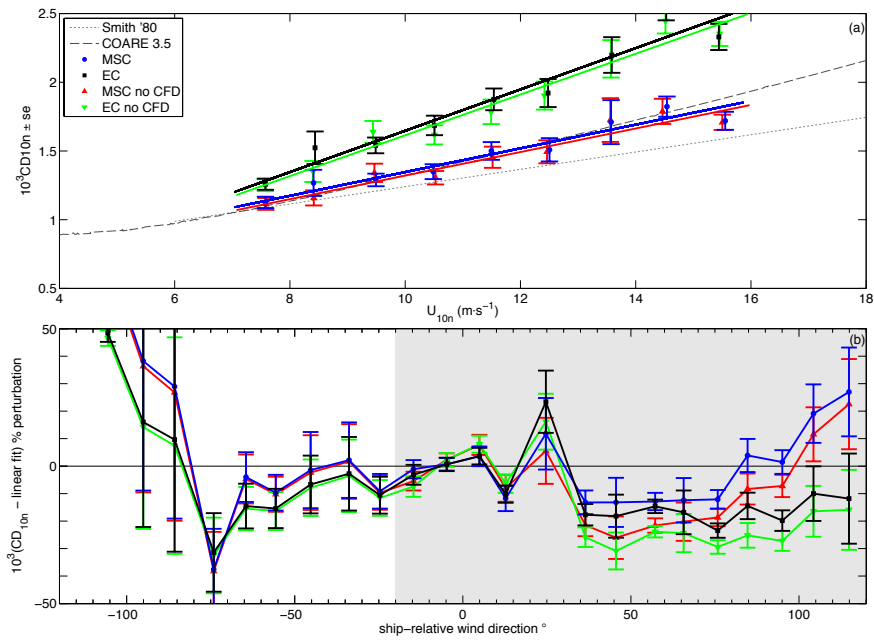
1013

1014

1015

Figure 5. Comparison of averaged spectra. In all panels two sets of averaged data are compared, periods when the ship was stationary ($V_{ship} < 1 \text{ m s}^{-1}$, 21 periods) and periods when the ship was steaming ($V_{ship} > 5 \text{ m s}^{-1}$, 20 periods); the individual spectra are shown as pale lines for reference. For all measurements, U_{10m} was between 10 and 12 m s^{-1} . (a) Spectral density of non-directional wave heights from WAVEX with frequency shifted to the reference frame of the moving ship; (b) spectral density of platform vertical velocity as measured on the foremast; (c) frequency-weighted inverted cospectral density for the momentum flux (positive upwards) – turbulent velocity components are motion corrected, but the MSC correction is not applied. The dashed vertical lines indicate the peak frequency of the wave spectrum; dotted vertical lines indicate the peak frequency of the momentum flux cospectra in (c). Note that the axis limits are set very close to the scale of the ship motion to allow details to be seen clearly.

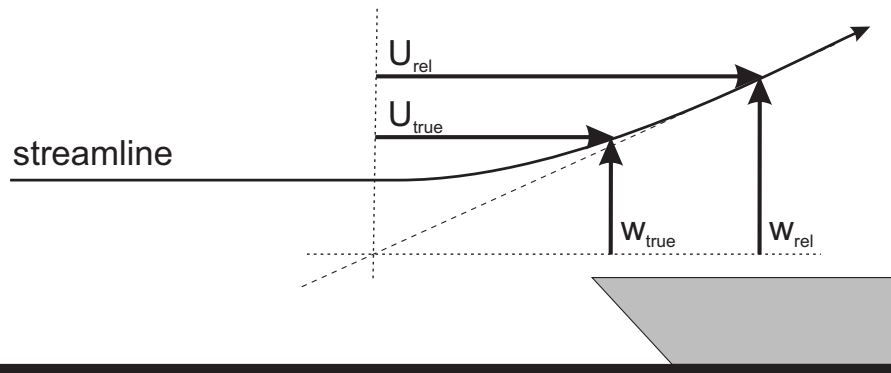
John Prytherch 3/9/2015 16:06
Deleted: ; (d) frequency-weighted cospectral density for the momentum flux calculated prior to motion correcting the turbulent velocity components.



1020

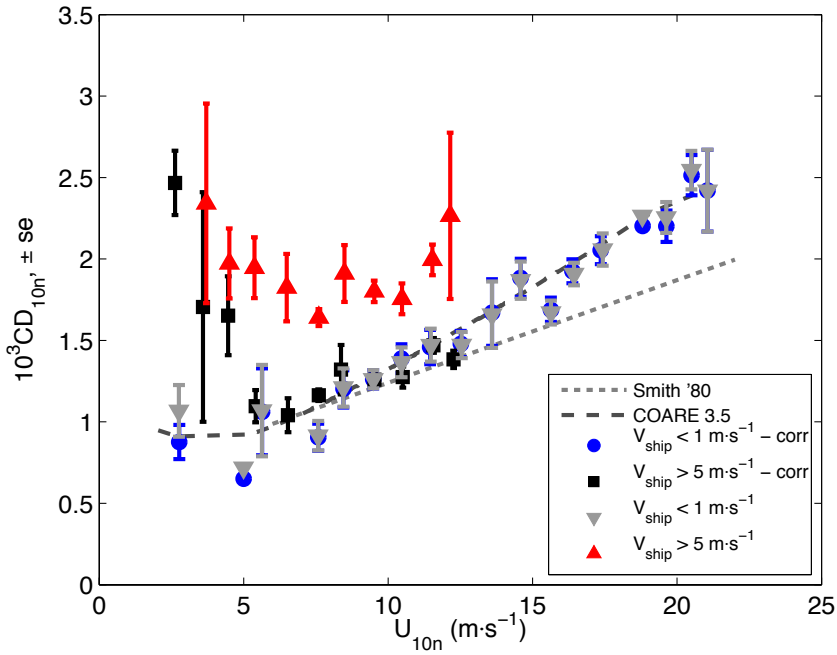
1021 Figure 6. (a): Measurements either without correction for wave-scale bias (EC), or with
 1022 correction applied to the vertical velocity only (MSC) for wind speeds $7 m s^{-1} < U_{10m} < 16 m$
 1023 s^{-1} ($n = 335$), and relative wind directions between -20° and $+50^\circ$ (where a wind on the bow
 1024 is at 0°). Lines are linear fits to the measurements. (b): variation of the difference between
 1025 measured drag coefficients and the linear fits against relative wind direction for the same
 1026 wind speed criteria ($n = 663$). Both panels also show measurements (with and without MSC)
 1027 which have not had CFD-derived corrections to mean wind speed and height applied. Note
 1028 that CFD corrections were only applied for the shaded range.

1029



1030

1031 Figure A1. Schematic of the impact of ship horizontal velocity on non-horizontal airflow.
1032 The measured horizontal (U_{rel}) and vertical (w_{rel}) wind components must both be corrected
1033 for ship velocity to obtain the true wind components. Not correcting the measured vertical
1034 wind will result in an incorrect determination of the tilt angle of the flow from horizontal.
1035



1037

1038

Figure A2. Wind speed-averaged drag coefficients, relative to U_{10n} . Two sets of measurements are compared: where the ship was deemed stationary ($V_{ship} < 1 m \cdot s^{-1}$, $n = 233$); and where the ship was underway ($V_{ship} > 5 m \cdot s^{-1}$, $n = 182$). The measurements are shown with ('corr') and without the vertical wind speed corrected as per Eq. (1).

1040

1041

1042